Fluorescent Immunological Paper-based Assay for Exosome detection

Surasak Kasetsirikul
Griffith University https://orcid.org/0000-0001-9767-1254
Muhammad J.A. Shiddiky (m.shiddiky@griffith.edu.au)
Griffith University https://orcid.org/0000-0002-9461-9888
Nam-Trung Nguyen (nam-trung.nguyen@griffith.edu.au)
Griffith University https://orcid.org/0000-0003-3626-5361

Research Article

Keywords: Exosome detection, Paper-based diagnostic device, Fluorescent-based assay

Posted Date: October 12th, 2021

DOI: https://doi.org/10.21203/rs.3.rs-963221/v1

Abstract

This paper reports the development of fluorescent-linked immunosorbent paper-based assay for exosome detection. The paper-based device was fabricated with sandwich lamination for easy handling and was coated with exosome-specific antibody as a biosensing platform to detect exosome sample from the cell culture media. This assay employed fluorescent detection which is followed by tagging fluorophore-conjugated detecting antibody on exosome samples. The fluorescent readout was evaluated and quantified from image processing software. This assay can detect high concentration of exosome samples (~ 10^{10} exosome/mL). However, this assay has encountered various challenges. First, the exosome concentration prepared from cell culture media from cancer-derived ovarian and mesothelial cell lines may be insufficient to reach detectable range. Second, chemical contamination from exosome isolation kits may affect assay sensitivity. Therefore, assay optimization and minimizing chemical contamination are required which could enhance assay specificity and sensitivity.

1. Introduction

Exosomes which are 30 – 150 nm in diameter are extracellular vesicles secreted from most cell types [1–5]. Many biomolecules such as proteins, lipids and various types of nucleic acids are found in exosomes. Ordinarily, exosomes are circulated in biological fluids such as saliva, blood, and urine. Many studies recommended that these exosomes play a significant role in cell-to-cell interaction and some pathological processes such as cancers [6], pregnancy complications [7, 8] and neurodegenerative diseases [9]. As such, during pregnancy, exosomes are one of signal pathways to communicate between the mother and the fetus [10]. During gestation, the human placenta releases exosome into the maternal circulation in the first trimester. Oxygen tension and glucose concentration including placental mass regulated the release of placental exosomes [11, 12]. There has been reported that the expected mothers, who have a higher concentration of placental-derived exosomes, face the risk of pregnancy complications such as gestational diabetes [8] and preeclampsia [7] than that of normal pregnancy. Therefore, detecting unusual level of placental-derived exosomes early as first trimester of pregnancy can help expectant mothers at risk to be treated properly before the complication develops.

Thus, the accurate purification and detection of exosomes from bodily fluids is still challenging [13]. Conventional methods such as gradient density centrifugation, ultrafiltration or immunological separation have been reported [14, 15]. However, these centrifugal isolations are time-consuming, and require expensive instrument and facilities, which may be inaccessible in poor-resource settings. Moreover, the commercial exosome isolation kit is also available. These kits shorten the process by precipitating exosome with polyethylene glycol or related chemicals, but the product may be contaminated with chemicals from the kits which possibly impact the downstream analysis. [16] Alternatively, flow cytometry [17, 18], nanoparticle tracking analysis (NTA) [19, 20], electrochemical-based method [21, 22], Enzyme-linked immunosorbent assay (ELISA) [23, 24] are successfully demonstrated to quantify and detect exosome. ELISA is known as a conventional method to detect and analyse various biomolecules, based on immunological affinity between antibodies and protein on exosome membranes.

However, the standard protocol is time consuming with laborious sample loading, washing, and incubation step.

Paper-based platform enables a number of microfluidic sample preparation tasks such as preconcentration and heating. [25, 26] Paper-based ELISA is a promising platform for diagnostic application due to the low cost, friendly use and small sample needed. This platform was successfully demonstrated for detecting antibodies and exosomes [27–30]. In limited-resource environments, colorimetric assay is useful and easily observed by naked eyes, however minor colour change may be difficult to differentiate due to the broad range of colour spectrum. [31] Fluorescent-linked immunosorbent assay (FLISA) promotes narrow detection range due to specific excitation and emission wavelength. Therefore, the present study developed FLISA paper-based assay for exosome detection. The exosome target was captured with exosome-specific antibody and formed immunological complex on the paper. The fluorescent readout relies on detecting emission photon excited by a specific wavelength, which results from immunological affinity between exosomes and fluorophore-conjugated antibody.

2. Materials And Methods

2.1 Materials and chemicals

Paper materials used as a platform device in this study were chromatography filter paper (CHR). Gloss laminate pouch with 80-µm thickness was used to make paper hydrophobic. For immunological assay, Rabbit monoclonal anti-human CD9 and CA125 monoclonal Anti-human (Anti-human CA125, MA1-24603, Invitrogen, USA) were used for coating and detecting antibody. AlexaFlour488-conjugation kit (ab236553, Abcam, UK) was used to conjugate AlexaFlour488 onto an antibody. Bovine Serum Albumin (BSA, A1595, Sigma Aldrich, USA) and Non-fat milk (NFM, Coles, Australia) were used to block the assay to minimize background signal due to non-specific binding. For exosome preparation, we used the same chemicals as described in the previous study. [32]

2.2 Paper-based device fabrication

Adapting from the previous study, we fabricated laminated CHR paper (L-CHR), Figure 1. Briefly, the device design was drawn by CorelDraw software and cut into 5-mm diameter piece using laser cutting machine including a laminated film which were cut with the hole of 4-mm diameter. Before the aligned paper-based device was fed into a laminator at a speed of 10 mm/s of 120^{o}C, the paper was aligned into the centre of laminated film hole. Finally, the paper-based device was cut into individual devices.

Figure 1 Schematic diagram of paper-based device fabrication

2.3 Experimental design and assay optimization

We employed sandwich FLISA assay on paper-based platform using immunoaffinity interactions. In this study, we used Anti-human CD9 as a primary antibody to capture all exosomes as CD9 was expressed and generic tetraspanin family of mammalian exosome membrane [33]. Anti-human CA125 was

commonly used as a biomarker to diagnose ovarian cancer [34, 35]. Thus, we selected Anti-human CA125 as a secondary antibody to capture ovarian cancer exosome. OVCAR3 exosome as of ovarian cancer cell lines was considered to be positive case and Met5a exosome as of mesothelial cell lines was considered to be negative case. PBS was used for control experiment by obtaining background signal and confirming the validity of the assay.

2.3.1 Secondary antibody concentration and incubation time optimization

According to our previous colorimetric immunological assay study, we selected 2% BSA for blocking [29]. However, concentration of fluorophore-conjugated anti-human CA125 and incubation time need to be optimized. In this study, 2% NFM was also evaluated. Briefly, 5 µL of 2% NFM blocking solution was added to incubate for 10 min and subsequently dry for 10 min. Then, we dropped anti-human CA125 tagged with AlexaFlour488 for 5 min onto the paper and washed subsequently. Subsequently, we put the paper device under fluorescent microscope and excite with light at a wavelength of 488 nm. We anticipated that the optimal condition for blocking could result in the lowest intensity of bright green colour.

2.3.2 Analytical performance of paper-based FLISA for exosome detection

In this study, we employed paper-based FLISA for exosome detection. Assay preparation and exosome preparation was adapted as described in the previous study [32]. Briefly, we dropped 5 µL of 0.1 mg/mL Rabbit anti-human CD9 on L-CHR paper and incubate for 10 min, then dry at 37^{o}C for 10 min. Next, a volume of 5 µL of 2% NFM solution was added to block and prevent non-specific absorption. In the presence of ovarian cancer exosome, AlexaFlour488-conjugated anti-human CA125 was left on exosome membranes as well as on the paper platform and was excited with light at the wavelength of 488 nm. The fluorophore molecules will emit green light. The intensity of the green fluorescence signal is proportional to the amount of excited photon. However, in the absence of ovarian cancer exosome, there was no AlexaFlour488-conjugated anti-human CA125 was left on the paper platform.

Furthermore, sample loading procedure was also investigated. We proposed two methods in the loading step. First, we performed the assay as our previous study which separates the step between loading sample and loading secondary antibody, Figure 2a. The exosome sample was incubated on L-CHR paper for 10 min, and the secondary antibody was loaded onto the paper for 20 min, respectively. Second, we incubated our exosomes with fluorophore-conjugated antibody solution before loading the mixture onto the paper, Figure 2b. The exosome sample was incubated in a secondary antibody solution for 30 min at room temperature. The mixture was loaded onto the paper and incubated for additional 10 min. Subsequently, the paper device was washed with PBS. Then, we placed the paper-based device under the fluorescent microscope and observed the emission of bright green signal when it was excited by the light at wavelength 488 nm.

2.4 Equipment setup and data acquisition

Due to the experimental result based on intensity of change from fluorophore, the paper device was observed under fluorescent microscope (Nikon Eclipse Ti-2, Nikon, Japan) with an excitation wavelength of 488 nm from light source (pE-4000, CoolLED, UK) and exposure time at 300 milliseconds. For image acquisition, the image was observed and recorded by an imaging software (NIS-Elements AR 5.00.00, Nikon, Japan). In the software, we can adjust LookUp Table (LUTs) which affects the colour output value. We set the range of LUTs value from 500 to 2,000 and 500 to 5,000 to show the best result of green signal observed under the microscope (see Supplementary Information section S.1). Image processing and quantification were performed with MATLAB.

2.5 Data processing and quantification

Qualitative data was observed as a bright green colour under excitation at the wavelength of 488 nm. All photos were processed and quantified with MATLAB. However, the fluorescent image emitted fluorescent signal at a wavelength of 525 nm which is green. Therefore, only the mean grey value (G) from the green channel was used to quantify the fluorescent signal. To confirm that the colour originates from the immunofluorescent assay, the value reported in this study was subtracted by the background signal from negative samples as:

$$G_{\text{value}} = G - G_{\text{neg}} \quad (1)$$

Where G is the mean gray value of the sample of interest, and G_{neg} is the mean grey value from negative sample. All experiments were individually performed with a sample number of at least $n = 3$. The error bar is determined by standard deviation.

3. Result And Discussion

3.1 Optimization of secondary antibody concentration and incubation time

Before performing the analytical assay for exosome detection by paper-based FLISA, we need to optimize concentration of fluorophore-conjugated antibody and incubation time as well as blocking solution. These two parameters are the main factors, which affect the assay performance. High fluorophore-conjugated antibody concentration and longer incubation time help promotes sensitivity, but could cause high background signal [36, 37]. We designed the experiment by varying the concentration of fluorophore-conjugated antibody from 1, 5 and 10 µg/mL and varying concentration time from 5, 10 and 20 minutes. Subsequently, all paper-based devices were observed under the fluorescent microscope and quantified by MATLAB. Figure 3 showed the fluorescent signal from various concentration of fluorophore-conjugated antibody under incubation at 5 min. The highest concentration up to 10 µg/mL can be used as it produced relatively low green fluorescent intensity. However, it may leave some contaminant small particles resulting from unfiltered PBS. In addition, Figure S.2 depicts the fluorescent signal from different

incubation time at a concentration of fluorophore-conjugated antibody of 10 µg/mL. The results showed that longer incubation up to 20 min still produced relatively low green fluorescent intensity. Therefore, based on this optimization, for analytical performance assay of exosome detection assay, we can select the fluorophore-conjugated antibody concentration at 10 µg/mL and incubation time up to 20 min as they produce relatively low background signal which could promote the immunological complex to form properly and produce the detectable signal for exosome detection. In addition to optimal conditions, LUTs value set by image acquisition software was selected with the scale of 500-2,000 as providing the widest range of green fluorescent signal.

3.2 Analytical performance assay

FLISA assay for exosome detection employs the presence of fluorophore-conjugated detecting antibody excited by a specific wavelength of the light source. To validate the exosome fluorescent immunological assay, we performed the analytical assay with a sample containing exosomes collected from ovarian cancer cell lines. On the contrary, a negative control sample is mesothelial, which is non-ovarian-cancer cell line. We investigated sample loading steps. Exosome concentration used in this investigate was 10^9 exosome/mL. Figure 5a depicts the fluorescent photos taken from the first method which is separately loading samples and fluorophore-conjugated secondary antibody. The G_{value} indicates that there is no significant difference and the negative control provide a bit higher signal comparing to the positive. Nevertheless, Figure 5b shows the fluorescent images taken from the second method, where exosome sample was incubated with fluorophore-conjugated secondary antibody before loading the mixture onto the paper. The G_{value} indicates that positive value provided a higher signal which was 5.746 (positive) vs 0.978 (negative). Therefore, we prepared the exosome sample by incubating with AlexaFlour488-conjugated anti-human CA125 for 30 min before loading onto the paper.

For analytical assay, we investigated concentration variation, which was 10^3, 10^6, 10^9, 10^{10} exosome/mL (Figure 6). The higher concentration of exosome sample can generate higher signal determined by G_{value}, while fluorescent readout seems not to produce significant difference by naked eye. Nevertheless, the result seems to be inconsistent due to sample and assay batch-to-batch variation. We repeated the experiment in each condition to obtain the average of G_{value} (Figure 7). However, the variation within the same exosome concentration may be too large to differentiate from other concentrations. Moreover, the exosome concentration may also be insufficient for FLISA method to produce green signal higher than a background signal.

4. Conclusion

We have developed and investigated a paper-based FLISA assay for exosome detection. Fluorescent readout facilitates high specificity of the readout due to specific wavelength emission and can be quantified by image processing. With the proof-of-concept, we optimized the assay and faced many challenges in assay development for detecting exosomes. First, exosome concentration from cell culture

may be insufficient for generating fluorescent emission signal in the detectable range. Second, the high background signal from non-specific binding and PEG contamination from exosome isolation kits may disturb the interaction between proteins [38]. In the future, this assay may require extensive optimization on assay operation to obtain better results.

Declarations

5. Acknowledgement

The authors acknowledge the support of the Australian Research Council (DP180100055) and higher degree research scholarships GUIPRS and GUPRS Scholarships to S.K. from the Griffith University.

The authors declare no competing interests.

References

1. Anand, P.K., *Exosomal membrane molecules are potent immune response modulators*. Communicative & integrative biology, 2010. **3**(5): p. 405–408.
2. Sokolova, V., et al., *Characterisation of exosomes derived from human cells by nanoparticle tracking analysis and scanning electron microscopy*. Colloids and Surfaces B: Biointerfaces, 2011. **87**(1): p. 146–150.
3. Valadi, H., et al., *Exosome-mediated transfer of mRNAs and microRNAs is a novel mechanism of genetic exchange between cells*. Nature Cell Biology, 2007. **9**(6): p. 654–659.
4. Soda, N., et al., *Advanced liquid biopsy technologies for circulating biomarker detection*. Journal of Materials Chemistry B, 2019. **7**(43): p. 6670–6704.
5. Boriachek, K., et al., *An amplification-free electrochemical detection of exosomal miRNA-21 in serum samples*. Analyst, 2018. **143**(7): p. 1662–1669.
6. Skog, J., et al., *Glioblastoma microvesicles transport RNA and proteins that promote tumour growth and provide diagnostic biomarkers*. Nature cell biology, 2008. **10**(12): p. 1470–1476.
7. Salomon, C., et al., *Placental Exosomes as Early Biomarker of Preeclampsia: Potential Role of Exosomal MicroRNAs Across Gestation*. The Journal of Clinical Endocrinology & Metabolism, 2017. **102**(9): p. 3182–3194.
8. Salomon, C., et al., *Gestational Diabetes Mellitus Is Associated With Changes in the Concentration and Bioactivity of Placenta-Derived Exosomes in Maternal Circulation Across Gestation*. Diabetes, 2016. **65**(3): p. 598.
9. *Alzheimer's disease β-amyloid peptides are released in association with exosomes.* Proceedings of the National Academy of Sciences, 2006. **103**(30): p. 11172.
10. Mitchell, M.D., et al., *Placental exosomes in normal and complicated pregnancy.* American Journal of Obstetrics and Gynecology, 2015. **213**(4, Supplement): p. S173-S181.

11. Rice, G.E., et al., *The Effect of Glucose on the Release and Bioactivity of Exosomes From First Trimester Trophoblast Cells*. The Journal of Clinical Endocrinology & Metabolism, 2015. **100**(10): p. E1280-E1288.
12. Salomon, C., et al., *Hypoxia-Induced Changes in the Bioactivity of Cytotrophoblast-Derived Exosomes*. PLOS ONE, 2013. **8**(11): p. e79636.
13. Lötvall, J., et al., *Minimal experimental requirements for definition of extracellular vesicles and their functions: a position statement from the International Society for Extracellular Vesicles*. Journal of Extracellular Vesicles, 2014. **3**(1): p. 26913.
14. Clayton, A., et al., *Analysis of antigen presenting cell derived exosomes, based on immuno-magnetic isolation and flow cytometry*. Journal of Immunological Methods, 2001. **247**(1): p. 163–174.
15. Merchant, M.L., et al., *Microfiltration isolation of human urinary exosomes for characterization by MS*. PROTEOMICS – Clinical Applications, 2010. **4**(1): p. 84–96.
16. van der Pol, E., et al., *Recent developments in the nomenclature, presence, isolation, detection and clinical impact of extracellular vesicles*. Journal of Thrombosis and Haemostasis, 2016. **14**(1): p. 48–56.
17. Erdbrügger, U. and J. Lannigan, *Analytical challenges of extracellular vesicle detection: A comparison of different techniques*. Cytometry Part A, 2016. **89**(2): p. 123–134.
18. Lacroix, R., et al., *Overcoming Limitations of Microparticle Measurement by Flow Cytometry*. Seminars in Thrombosis and Hemostasis, 2010. **36**(8): p. 807–818.
19. Dragovic, R.A., et al., *Sizing and phenotyping of cellular vesicles using Nanoparticle Tracking Analysis.* Nanomedicine: nanotechnology, biology, and medicine, 2011. **7**(6): p. 780-788.
20. Soo, C.Y., et al., *Nanoparticle tracking analysis monitors microvesicle and exosome secretion from immune cells*. Immunology, 2012. **136**(2): p. 192–197.
21. Boriachek, K., et al., *Avoiding Pre-Isolation Step in Exosome Analysis: Direct Isolation and Sensitive Detection of Exosomes Using Gold-Loaded Nanoporous Ferric Oxide Nanozymes*. Analytical Chemistry, 2019. **91**(6): p. 3827–3834.
22. Yadav, S., et al., *An Electrochemical Method for the Detection of Disease-Specific Exosomes*. ChemElectroChem, 2017. **4**(4): p. 967–971.
23. Khan, S., et al., *Early diagnostic value of survivin and its alternative splice variants in breast cancer*. BMC Cancer, 2014. **14**(1): p. 176.
24. Logozzi, M., et al., *High Levels of Exosomes Expressing CD63 and Caveolin-1 in Plasma of Melanoma Patients*. PLOS ONE, 2009. **4**(4): p. e5219.
25. Dinh, T., et al., *Graphite on paper as material for sensitive thermoresistive sensors*. Journal of Materials Chemistry C, 2015. **3**(34): p. 8776–8779.
26. Phan, D.-T., et al., *Sample concentration in a microfluidic paper-based analytical device using ion concentration polarization*. Sensors and Actuators B: Chemical, 2016. **222**: p. 735–740.

27. Chen, C., et al., *Paper-based devices for isolation and characterization of extracellular vesicles*. Journal of visualized experiments: JoVE, 2015(98): p. e52722-e52722.
28. Cheng, C.-M., et al., *Paper-Based ELISA*. Angewandte Chemie International Edition, 2010. **49**(28): p. 4771–4774.
29. Kasetsirikul, S., et al., *Detection of the SARS-CoV-2 humanized antibody with paper-based ELISA*. Analyst, 2020. **145**(23): p. 7680–7686.
30. Lee, J., et al., *Enhanced paper-based ELISA for simultaneous EVs/exosome isolation and detection using streptavidin agarose-based immobilization*. Analyst, 2020. **145**(1): p. 157–164.
31. Sapan, C.V., R.L. Lundblad, and N.C. Price, *Colorimetric protein assay techniques*. Biotechnology and Applied Biochemistry, 1999. **29**(2): p. 99–108.
32. Kasetsirikul, S., M.J.A. Shiddiky, and N.-T. Nguyen, *Colorimetric Immunological Paper-based Assay for Exosome Detection.* 2021.
33. Boriachek, K., et al., *Biological Functions and Current Advances in Isolation and Detection Strategies for Exosome Nanovesicles*. Small, 2018. **14**(6): p. 1702153.
34. Dochez, V., et al., *Biomarkers and algorithms for diagnosis of ovarian cancer: CA125, HE4, RMI and ROMA, a review*. Journal of Ovarian Research, 2019. **12**(1): p. 28.
35. Scholler, N. and N. Urban, *CA125 in ovarian cancer*. Biomarkers in Medicine, 2007. **1**(4): p. 513–523.
36. Cooperation, E.M., *Rapid Lateral Flow Test Strips: Consideration for product development*. 2013.
37. Wong, R. and H. Tse, *Lateral Flow Immunoassay*. 1 ed. 2009: Humana Press. 224.
38. Patel, G.K., et al., *Comparative analysis of exosome isolation methods using culture supernatant for optimum yield, purity and downstream applications*. Scientific Reports, 2019. **9**(1): p. 5335.

Figures

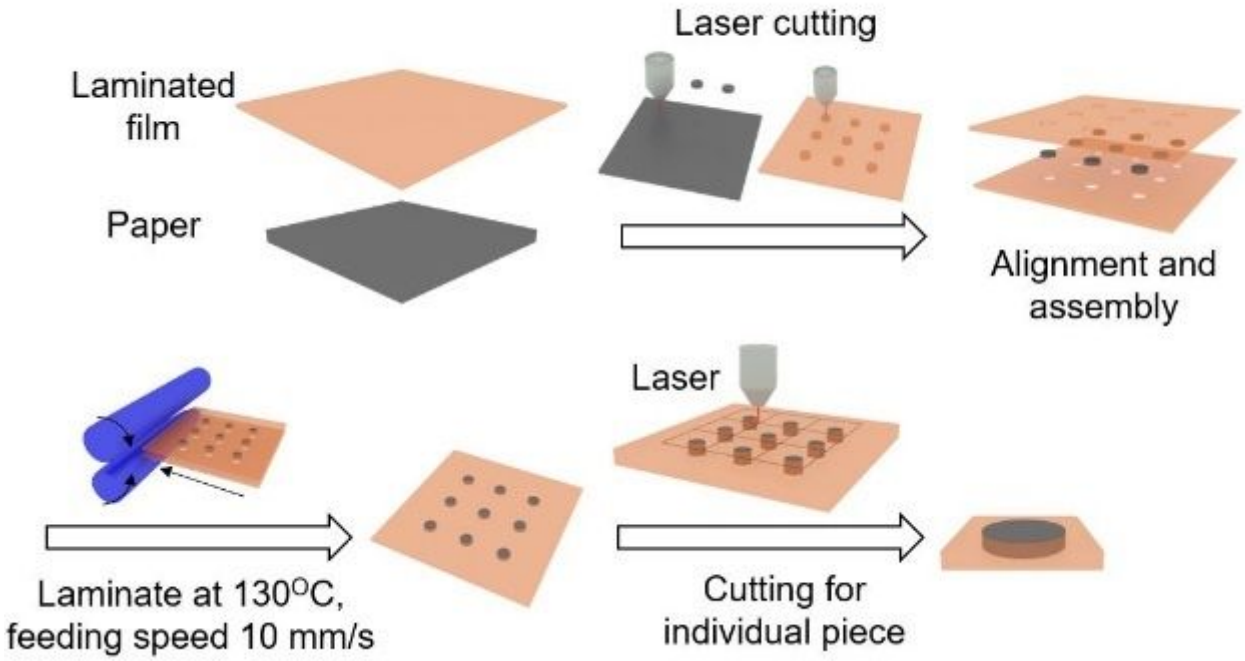

Figure 1

Schematic diagram of paper-based device fabrication

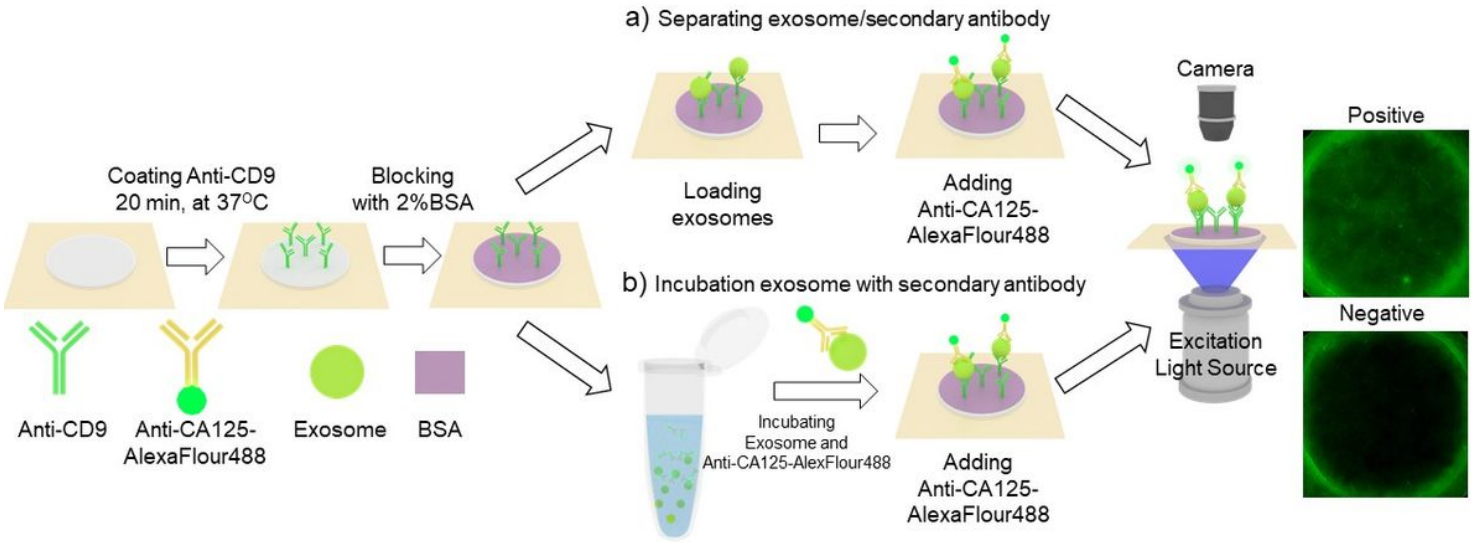

Figure 2

Schematic diagram of assay preparation and optimization: (a) separately loading exosome sample and secondary antibody solution; (b) incubating exosome sample with secondary antibody before loading the mixture onto the paper.

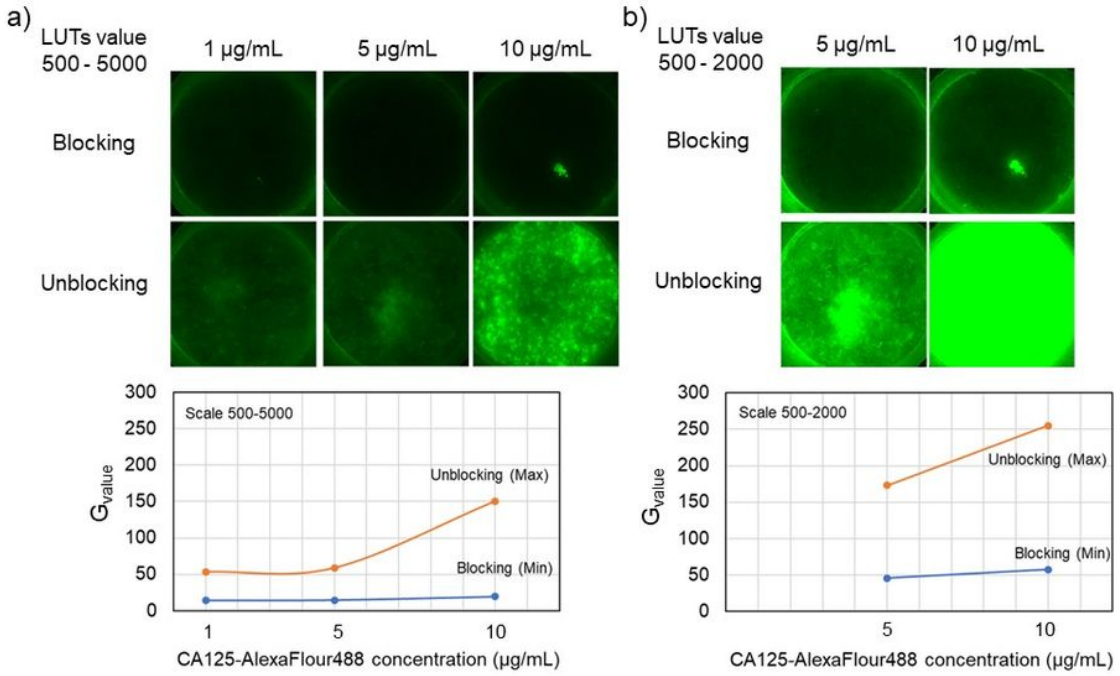

Figure 3

Optimization of secondary antibody concentration. Images of Green fluorescent intensity with various concentrations (1 – 10 µg/mL) of fluorophore-conjugated antibody under incubation for 5 min with line graph of mean grey value quantified from images: (a) LUTs values 500 – 5,000; (b) LUTs values 500 – 2,000.

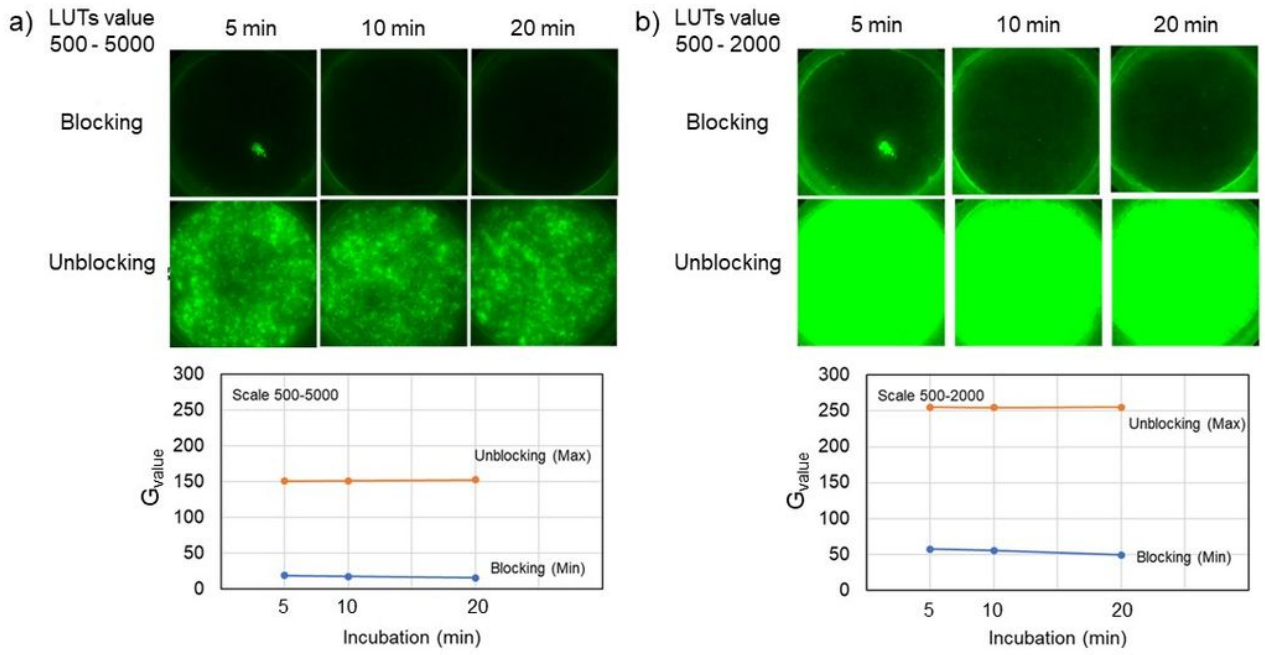

Figure 4

Optimization of secondary antibody incubation time. Images of Green fluorescent intensity with incubation time (5 – 20 min) of fluorophore-conjugated antibody under concentraion of 10 µg/mL with line graph of mean grey value quantified from images: (a) LUTs values 500 – 5,000; (b) LUTs values 500 – 2,000.

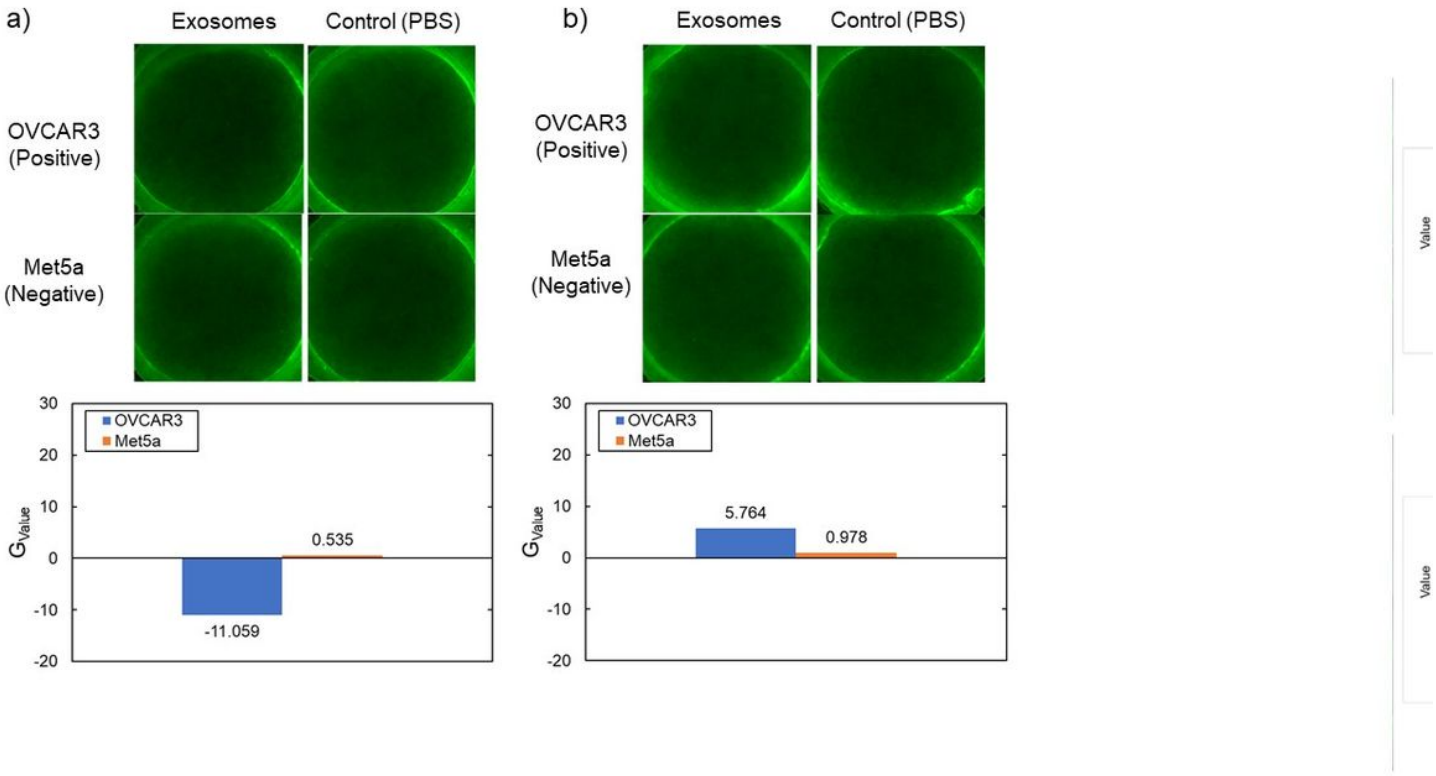

Figure 5

Analytical performance for sample loading step for exosome detection (109 exosome/mL) including bar diagram of GValue (a) with the separately loading exosome sample and secondary antibody and (b) with mixture between exosome sample and secondary antibody.

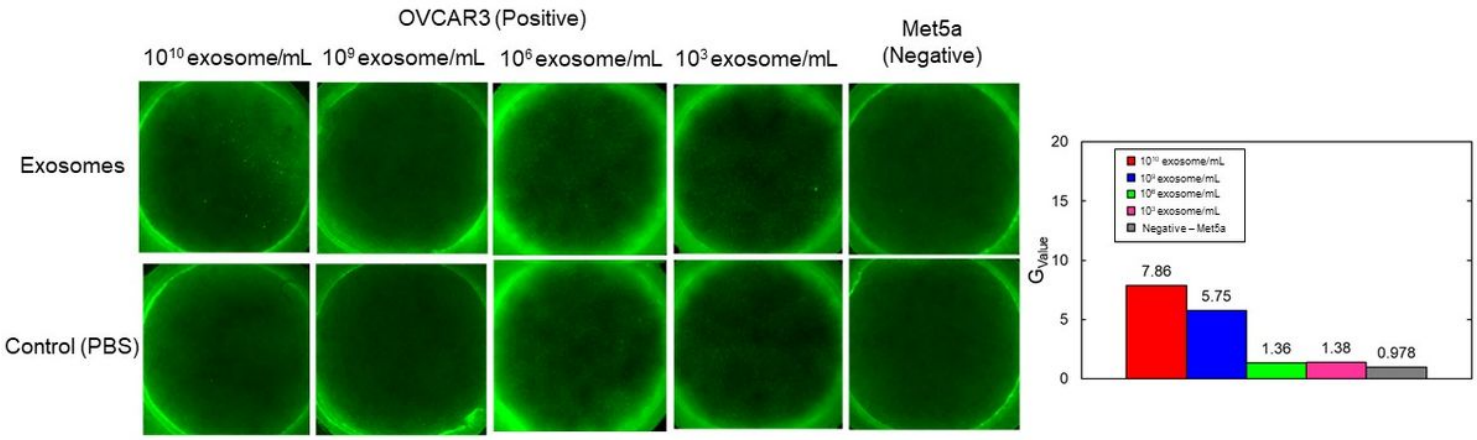

Figure 6

Assay sensitivity. Sequential images of FLISA assay for exosome detection with different exosome sample concentrations (103, 106, 109, 1010 exosome/mL) with bar diagram of Gvalue quantified from images

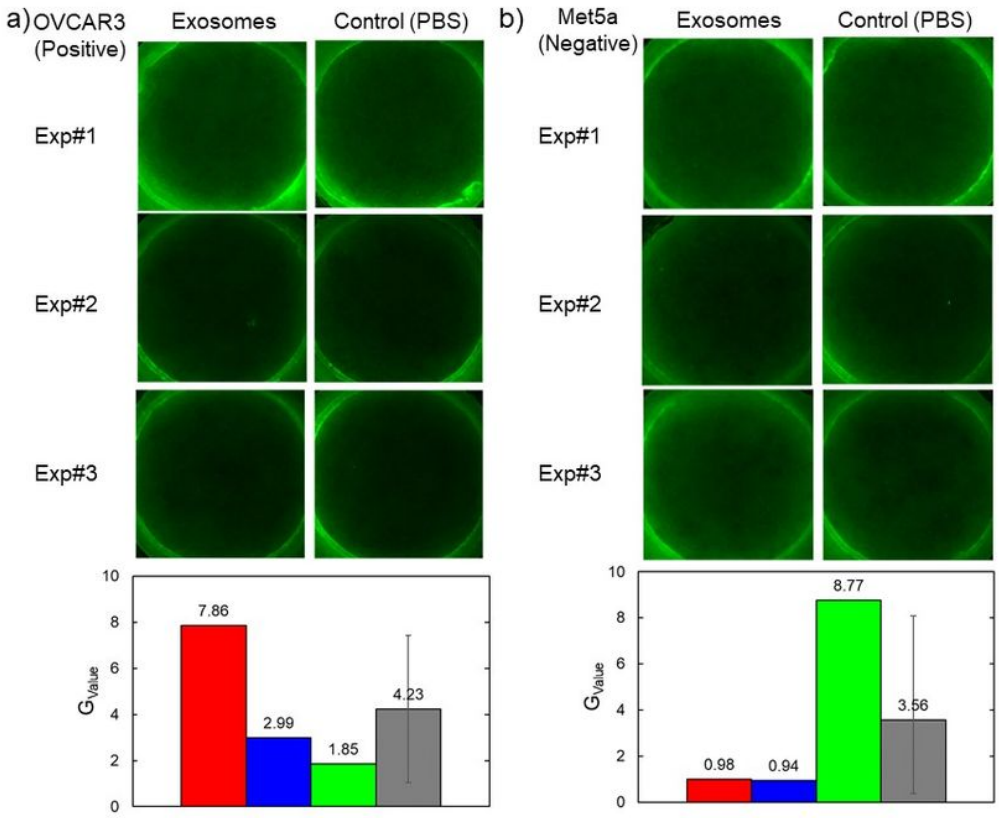

Figure 7

Assay repeatability. Sequential images of FLISA assay for exosome detection (109 exosome/mL) with individual experiment with bar diagram of Gvalue quantified from images: (a) positive sample (OVCAR3) (b) negative sample (Met5a)

Supplementary Files

This is a list of supplementary files associated with this preprint. Click to download.

- supplementaryinformation.docx